Duality-Derived Transformer Models for Low-Frequency Electromagnetic Transients—Part II: Complementary Modeling Guidelines

S. Jazebi, *Senior Member, IEEE*, A. Rezaei-Zare, *Senior Member, IEEE*, M. Lambert, *Member, IEEE*, S. E. Zirka, N. Chiesa, Y. I. Moroz, X. Chen, *Member, IEEE*, M. Martinez-Duro, *Member, IEEE*, C. M. Arturi, *Member, IEEE*, E. P. Dick, *Senior Member, IEEE*, A. Narang, *Senior Member, IEEE*, R. A. Walling, *Fellow, IEEE*, J. Mahseredjian, *Fellow, IEEE*, J. A. Martinez, *Senior Member, IEEE*, and F. de León, *Fellow, IEEE*

***Abstract*—This two-part paper is intended to clarify definitions in dual transformer modeling that are vague, provide accurate modeling guidelines, clarify misconceptions about numerical instability, provide a unified dual model for a specific type of transformer, and introduce new paths of research to the power systems/electrical machinery community for low-frequency transients. Part I discussed the topology of duality-based models and some important issues, such as the most common approaches to derive dual models and their variety, the equivalence of negative inductance and mutual couplings to represent the leakage inductance of three-winding transformers, and the numerical oscillations caused by the use of nontopological models. This part of the paper discusses and compares white-, gray-, and black-box models. The paper also reviews hysteresis models (static and dynamic) and highlights the differences between the air-core inductance and saturation inductance. The available dual models for the representation of the transformer tank are then presented. A unified and accurate model of a three-phase core-type transformer adequate for all low-frequency transients is presented. Finally, concrete guidelines are presented for the appropriate selection of the model topology and parameters for different low-frequency transient studies.**

***Index Terms*—Duality models, electromagnetic transients, modeling guidelines, tank models, transformer modeling.**

Manuscript received November 29, 2015; revised March 1, 2016; accepted April 18, 2016. Date of publication April 22, 2016; date of current version September 21, 2016. Paper no. TPWRD-01654-2015.

S. Jazebi and F. de León are with the Department of Electrical and Computer Engineeringat , New York University, Brooklyn, NY 11201 USA (e-mail: jazebi@ieee.org; fdeleon@nyu.edu).

A. Rezaei-Zare and A. Narang are with Hydro One Networks Inc., Toronto, ON, M5G 2P5, Canada (e-mail: Afshin.Rezaei-Zare@HydroOne.com; arun.narang@ieee.org).

M. Lambert and J. Mahseredjian are with the Department of Electrical Engineering, École Polytechnique de Montréal, Montréal, QC H3T 1J4 Canada (e-mail: mathieu.lambert@polymtl.ca; jean.mahseredjian@polymtl.ca).

S. E. Zirka and Y. Moroz are with the Department of Physics and Technology, Dnepropetrovsk National University, Dnepropetrovsk 49050, Ukraine (e-mail: zirka@email.dp.ua).

N. Chiesa is with Statoil, Trondheim NO-7005, Norway (e-mail: nchie@statoil.com).

X. Chen is with the Department of Electrical Engineering, Seattle University, Seattle, WA 98122 USA (e-mail: xchen@seattleu.edu).

M. Martínez-Duró is with Électricité de France R&D, Clamart 92141, France (e-mail: manuel.martinez@edf.fr).

C. M. Arturi is with the Department of Electronics, Information and Bioengineering, Politecnico di Milano, Milan 20133, Italy (e-mail: cesaremario.arturi@polimi.it).

E. P. Dick is with Kinectrics Inc, Toronto, ON M8Z 5G5 Canada (e-mail: epdick@ieee.org).

R. A. Walling is with Walling Energy Systems Consulting, LLC, Clifton Park, NY 12065-1622 USA (e-mail: rwalling@wesconsult.com).

J. A. Martinez is with the Departament d'Enginyeria Elèctrica, Universitat Politècnica de Catalunya, Barcelona 08028, Spain (e-mail: jamv@ieee.org).

Color versions of one or more of the figures in this paper are available online at http://ieeexplore.ieee.org.

Digital Object Identifier 10.1109/TPWRD.2016.2556686

I. Introduction

TOPOLOGICAL duality-based transformer models have been discussed in Part I of this paper. Although the modeling principles have been known for a long time, Part I was intended to dispel lingering misconceptions in the industry. This Part II is focused on art that is not mature and discusses topics still very much under research. Hence, this paper is aimed at reviewing the recent progress in the art of transformer modeling and to introduce new horizons for future research in this field.

The paper starts with an introduction and comparison of the so-called white-, gray-, and black-box models. Different available methods to compute the parameters for any of these models are summarized.

The proper representation of the iron-core structure of transformers is crucial for the study of low-frequency transients. The physical behavior of the iron is non-linear and frequency dependent, so dynamic hysteresis models (frequency and voltage dependent) are required for the accurate simulation of some low-frequency transients.

Commonly, the terms "air-core inductance" and "saturation inductance" are misinterpreted. It is discussed in the next section why the term "saturation inductance" is preferred to refer to the saturation region of the magnetizing characteristic of a transformer.

Nowadays, the modeling techniques for the transformer tank are under investigation. Several models have been proposed for the representation of the tank. This paper summarizes duality-based models for representing the transformer tank, and analyzes their scopes and limitations.

Power system transients are commonly identified by their frequency. Ferroresonance, geomagnetically induced current (GIC), harmonic, and inrush current studies are classified as low-frequency transients, since these phenomena involve frequencies of less than 3 kHz (below the windings' first resonance) [1]. These studies require accurate representation of particular transformer features. The paper presents a discussion on the importance of the different model components and their relative

influence in a particular transient study. Then, concrete guidelines are presented for the appropriate selection of the model topology and parameters.

II. Classification of Transformer Models and Calculation of Their Parameters

Transformer models, despite the scope and limitations, can be categorized into three main subcategories: white-, black-, or gray-box equivalents [2]. The parameters of these models can be identified either from the geometry and material information of the transformer, from terminal measurements, from measurements and mathematical fitting methods, or a hybrid approach consisting of measurements, geometrical data, and fitting techniques. This section is aimed to clarify the scopes, limitations, differences, drawbacks and advantages of these models. The main idea is to give insight into the selection of a proper model for a specific application.

A. Black-Box

Black-box models take advantage of mathematical identification methods to fit the terminal behavior of transformers with respect to field measurements (either time domain and/or frequency-domain data) [3]. These models accurately replicate the terminal response of the transformer under study. However, this approach does not provide information regarding the internal behavior of the transformer. Also, the models are not general for all operating conditions. For example, a high-frequency model for the leakage inductance in short circuit condition cannot represent the open circuit behavior of the transformer. This is so because the parameters of the models are calculated for a specific condition utilizing the corresponding measurements. Therefore, different black-box models need to be produced for different situations. The alternative is to merge two separate methods with special schemes such as filters [4]. Nevertheless, these models have been generally applied for mid- and high-frequency applications, and are not popular for the purpose of representation of low-frequency transients.

B. White-Box

White-box models are usually built from basic electrical components such as inductors, resistors, capacitors, etc. These components correspond to physical parts of the transformer structure and usually carry a physical meaning. White-box models are built based on the knowledge of the internal geometry and material properties [5]–[9]. The main drawback of the white-box models is the need to gain access to the actual transformer dimensions and design details. This information, however, is proprietary of the manufacturer and is never available.

In addition, many transformers currently in use in power systems are relatively old (with average age of about 40 years [10]). Hence, the relevant design data for these transformers is challenging to get; if not impossible. The restricted access to the design documentation makes the construction of a white box model outside the laboratory or a manufacturing firm a serious problem. Thus these methods are mainly suitable for manufacturers or transformer designers.

The major advantage of white-box models is that they allow for the detailed analysis of the internal overvoltages, the estimation of the distribution of the magnetic flux, and the prediction of the eddy currents and losses in different regions of the transformer geometry. Therefore, the obtained circuit can give an accurate understanding of the electromagnetic behavior of the transformer components at different frequencies and operating conditions. This makes the model an ideal tool to design magnetic components. For example, a detailed model could be synthesized to represent the transformer magnetic and capacitive effects. This would allow to take into account the distribution of the voltage across the insulation of the windings for a wide range of frequencies, e.g., to predict the insulation behavior during switching or impulse transient voltages. White-box models are helpful for the design of the transformer insulation system [11].

C. Gray-Box

Perhaps the more practical models, a compromise between the black- and white-box models, are the so-called gray-box models, see for example [11]–[16], which may be fairly accurate and retain some physicality. The topology and the structure components are derived physically as for white-box models. However, the model parameters are estimated from terminal measurement data, such as saturation inductance measurements, as for black-box models. Nowadays, many transformer modelers are showing interest in gray-box models. The gray-box modeling techniques overcome the limitations associated with access to the transformer's construction and material information. However, the main challenge is to estimate the parameters from terminal measurements [2], [11], [13].

III. Hysteresis Modeling

In the context of transformer modeling, hysteresis is one of the most complicated phenomena to model as it is a nonlinear, history- and frequency-dependent phenomenon.

Iron core losses in grain-oriented (GO) steel, the predominant transformer core material, can be divided into three general categories: static hysteresis (which account for about 40% of the total), classical eddy current (about 20%), and excess losses (about 40%) [17]–[19]. The term excess loss reflects the fact that it is anomalous from the viewpoint of the classical loss theory [20], which is mainly applied to non-oriented ("dynamo") steels used in generators and motors. Based on how the iron core models account for the loss components, two types of hysteresis models exist: static and dynamic.

A. Static Hysteresis Models

The purpose of static hysteresis models is to reproduce the major hysteresis loop as well as to predict any symmetrical or asymmetrical minor loops at zero frequency [21]. The simplest forms are history-independent hysteresis models (HIHMs), such as Jiles-Atherton [22]. This model build trajectories

independent of the magnetization history (i.e., of the previous reversal points). More realistic (but complex) models are history-dependent hysteresis models (HDHMs), such as Preisach [23]. This model reproduces the magnetization history. In particular, the HDHMs construct minor loops, which are immediately closed. An extensive review of static hysteresis models can be found in [24].

An important phenomenon observed in the hysteretic behavior is the changes of hysteresis loop with voltage amplitude and frequency, and thus the variation of the core loss in each cycle. The conventional method to simulate this behavior is to include a resistor in parallel with the hysteresis inductor. This resistance needs to be adjusted for different excitations.

During a number of transients such as ferroresonance, GIC, inrush, etc., the terminal voltages differs from sinusoidal. In this condition, the excitation changes both in the amplitude and frequency. Besides, for example, even at a sinusoidal excitation, the fluxes in the yokes and lateral limbs of the five-limb transformers are substantially non-sinusoidal. In all these cases, a more accurate method is required that dynamically (self-adaptively) represent the variation of the core losses.

B. Dynamic Hysteresis Models

The total loss in conducting ferromagnetic laminations depends not only on the flux density, but also on the magnetization frequency and hence on the voltage waveform. The aim of a composite dynamic hysteresis model (DHM) is to model different frequency and voltage dependencies of each individual loss components. A DHM is rate-dependent that means the area of hysteresis loop increases with increments in frequency and voltage. A dynamic hysteresis model can be represented based on the contributions of all magnetization attributes as follows:

$$W_{\mathrm{tot}} = W_{\mathrm{hys}} + W_{\mathrm{eddy}} + W_{\mathrm{exc}} \tag{1}$$

where the total power loss W_{tot} is obtained by adding the static hysteresis loss W_{hys}, eddy current loss W_{eddy}, and excess loss W_{exc}. It can be shown [25] that the separation of the total loss into the components (static hysteresis, eddy currents, and excess losses) is equivalent to the separation of the magnetic field $H\,(t)$ into corresponding magnetic field components:

$$H\,(t) = H_{\mathrm{hys}}\,(B) + k_{\mathrm{eddy}}\frac{dB\,(t)}{dt} + g\,(B)\left|\frac{dB\,(t)}{dt}\right|^{0.5}\delta \tag{2}$$

The field $H_{\mathrm{hys}}\,(B)$ is calculated using an inverse hysteresis model, the eddy current constant $k_{\mathrm{eddy}} = d^2/\,(12\rho)$ is determined by the resistivity ρ of the core material and the lamination thickness d, the directional parameter $\delta = \pm 1$ for the ascending and descending hysteresis branches respectively, and function $g\,(B)$ controls the shape of dynamic hysteresis loop. Typically, dynamic loops of GO steel are narrower for smaller flux densities (around the waist) and become wider towards the knee. The simplest form of $g\,(B)$ (to get a minimum at lower $|B\,(t)\,|$ and a maximum for higher $|B\,(t)\,|$) is a polynomial given by [19]:

$$g\,(B) = k_1\left(1 + k_2 B^2\right) \tag{3}$$

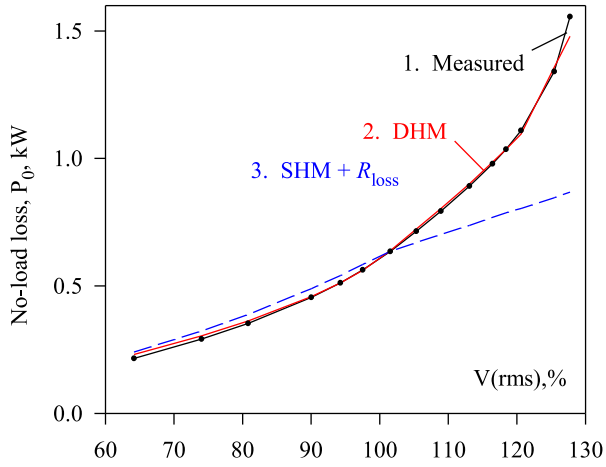

Fig. 1. No-load losses in a 300 kVA transformer. Curve 2 represents the losses calculated with DHM according to (2); curve 3 shows the losses predicted using SHM in parallel with a constant resistor [27].

where constant k_1 governs the waist and area of the dynamic loop, and constant k_2 controls its shape (makes it wider when approaching saturation).

In the duality-derived implementation of the DHM, the second and the third terms of (2) can be represented by linear and nonlinear resistors respectively [26].

Applications of an accurate hysteresis model include the estimation of the residual flux in transformer limbs. The role of $g\,(B)$ in (2) has been recently demonstrated in [27] where DHM-inductors are used in the model of a 300 kVA three-phase transformer. The no-load losses are correctly estimated for a wide range of terminal voltages (see curve 2 in Fig. 1). Curve 3 illustrates the limitations of the traditional method to represent the iron core losses. This is the static hysteretic (or non-linear) inductor in parallel with resistor R_{loss}, which are obtained using only the hysteretic (SHM) and eddy current components (R_{loss}) in (2). Here, to compensate for the absence of the excess field, the value of k_{eddy} was enlarged to match the open circuit losses at *nominal* voltage. One can see from Fig. 1, that the inaccuracy of this simplified method (when neglecting the excess losses) increases rapidly when $V > 1$ pu.

IV. Saturation and Air-Core Inductance

There is often a misconception in the literature about the terms "air-core inductance" and "saturation inductance", where both are sometimes assumed to have the same meaning. These terms have also been referred as "incremental" inductance and "apparent" inductance in the literature [28]. The air-core inductance is, as the name implies, the inductance that would be measured across a winding (with all other windings opened, including deltas) as if the ferromagnetic core (and all surrounding ferromagnetic material) did not exist. Then, the inductance would be equivalent to the self-inductance of the winding in air [29].

In contrast, the term "saturation inductance" should be reserved for the line with the lowest slope of a nonlinear inductor during a transient that starts at λ_0 in the flux-linkages versus

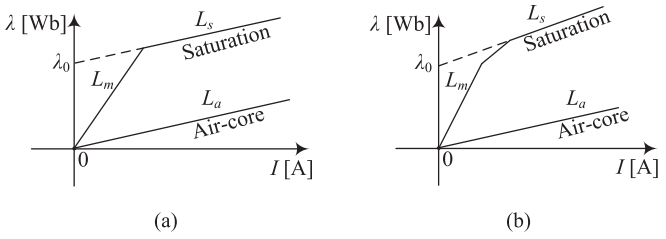

Fig. 2. Comparison of the air-core and terminal saturation inductance: (a) case where the slopes are equal; (b) case where the slopes are different.

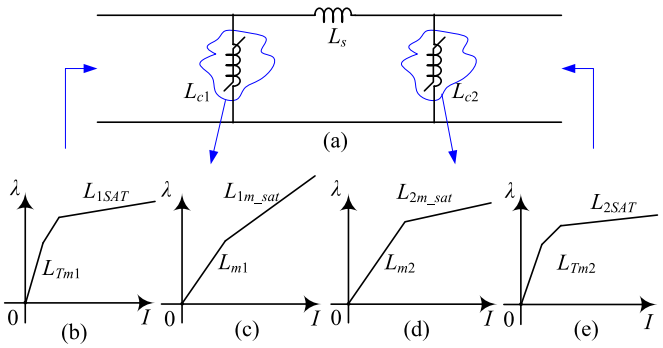

Fig. 3. Comparison of component saturation inductance and terminal saturation inductance; (a) simplified π model for a shell-type transformer with piecewise linear components to represent the iron core; (b) terminal saturation inductance seen from winding 1; (c) component saturation inductance to represent the leg; (d) component saturation inductance to represent the yoke; (e) terminal saturation inductance seen from winding 2.

current characteristic (see Fig. 2). Thus, the value of the saturation inductance depends on the particular topology of the transformer under study and its accessories such as tank and shunts that are involved in the saturation. These definitions are in agreement with the observations in [30]. Since the saturation inductance is measured from the terminal of the transformer, in this paper, it is called the "terminal saturation inductance."

Each topological transformer model consists of several components (nonlinear/linear inductors). Take for example the simplified π model of Fig. 3. The nonlinear components (L_{c1} and L_{c2}) can reach their saturation point at different excitation levels. The term saturation inductance has been used to describe the saturation condition of these individual components in [29]. In this paper, these characteristics are called the "component saturation inductance." The "terminal" and "component" saturation inductances are not equivalent. The terminal saturation inductances are the equivalent inductances that can be calculated from the values of the component saturation inductance and other transformer parameters such as leakage inductance as can be seen in Fig. 3.

In the extreme circumstance, when all elements in the transformer have reached their "component" saturation inductance, the slope of the "terminal" saturation inductance is equal to the air-core inductance. This is shown in Fig. 2(a). However, generally, because of the existence of tank, shunts, shields, wires, etc., these two slopes are not equal, as shown in Fig. 2(b). The transformer accessories often do not saturate at the same magnetic flux density. For example, shunts and tank often saturate at different levels of flux. Therefore, in reality, the terminal $\lambda - i$ curve does not consist of two straight lines. In fact, it has a continual transition from L_m to L_s. The simplest representation is a curve with three slopes, shown in Fig. 2(b).

In conclusion, for a specific transformer winding, the air-core inductance is always constant. However, the terminal inductance may or may not be equal to air-core inductance. The saturation inductance is a function of the geometry of the core and windings, and transformer accessories such as tank, shunts, clamping, etc.

V. Transformer Tank Modeling

Often a significant amount of flux will find a path through the tank and/or magnetic tank shunts under core saturation conditions; i.e., over-excitation for all transformer types. Additionally, the tank especially affects the behavior of three-phase transformers under the existence of zero-sequence currents and over-excitation. Therefore, an accurate tank model needs to represent the correct behavior for balanced and unbalanced over excitation conditions. The model should properly represent the induced currents from nearby conductors and from conductors that cross the structure. Note that the tank may have shielding that also needs to be modeled.

A. Single-Phase Transformers

For single-phase transformers, the presence of the tank changes the value of the corresponding component saturation inductance and consequently there is a variation of the terminal saturation inductance of the model. The topology of the reversible π-model presented in Part I does not change when the tank exists, but the values of the saturation parameter of the model need to be properly computed. For this purpose, measurements under saturation conditions are needed. Independently of the geometry of the core and the tank, the "terminal saturation inductance" can be accurately measured from terminal measurements [31]–[35].

A parametric study is carried out on the 1 kVA shell-type transformer described in the Part I. This is the single-phase, 4-winding, shell-type transformer studied in [12], where its full geometrical information is presented. The transformer is modeled in 3D finite element software with and without its tank. Eddy current effects are not considered in the simulations. The terminal saturation inductance is calculated from the magnetic energy of the complete domain. The simulation results are compared in Table I. These results show that the terminal saturation inductance is larger for transformers with tank when the tank is not saturated. This is so because the magnetic flux closes through the tank with higher permeability than air. Also, the flux paths change in the presence of the tank (the mean flux paths lengths reduce). If the tank saturates, the magnetic flux passes through the walls as if it were air. Therefore, the terminal saturation inductance when the tank is saturated is equivalent to the saturation inductance of the transformer without tank.

Studies have been carried out for tanks with larger dimensions (larger clearance between tank wall and winding/core) for

TABLE I
COMPARISON OF TERMINAL SATURATION INDUCTANCE OF A 4-WINDING SINGLE-PHASE TRANSFORMER WITH AND WITHOUT TANK

Winding	L_s without tank (μH)	L_s with tank (μH)	Difference (%)
1	645	685.9	5.96
2	850	922.7	7.88
3	1069	1181	9.48
4	1300	1460	10.96

the same transformer. The conclusion of those studies is, as expected, that the terminal saturation inductance decreases when the tank dimensions increase. This is so because, in a transformer without enclosure, the magnetic flux closes its path through air. However, in the presence of a tank, the stray flux lines are perpendicular to the surface of the tank and consequently close their path through the tank. The percent difference of terminal saturation inductance with and without the tank may change for larger transformers. However, the conclusion of the study is generally valid for single-phase transformers.

The above mentioned circumstances are valid when transformers tanks have shields to prevent eddy current effects. If the magnetic effects of the induced eddy currents are taken into account (for tanks without magnetic shields), the final slope of the terminal saturation inductance may be even lower than the air-core inductance. This is so because the equivalent inductance (at terminals) includes now (one or more) short-circuited inductors in series.

B. Three-Phase Transformers

The tank model for three phase transformers needs to represent the zero sequence impedance Z_0 for unbalanced cases as well as the correct behavior during over-excitation. Note that in over-excitation, the effect of the tank is significant for any kind of transformer and winding connection, for inrush currents and GIC. However, zero sequence impedance representation needs more considerations, as described next.

The influence of the tank is mainly significant for core type, three-legged transformers without delta-connected windings. The zero sequence impedance can be obtained from zero sequence tests in which a *single-phase* voltage is applied to the three phases (connected together) and the neutral. The same excitation exposed to all three legs compels the flux to leave the core and find a return path through the air and tank. The low reluctance of the core legs is negligible when compared to the high reluctance of air and inner layers of the tank walls. The flux cannot penetrate into conducting steel (thick walls) at 50/60 Hz and at a low excitation voltage. However, when the voltage increases, the zero-sequence flux increases proportionally and penetrates deeply into the tank walls [36], and in addition may saturate different parts of the tank, shunts, and structural components [16]. This changes the reluctance of the zero-sequence flux path and hence the impedance Z_0 measured at the terminals. The values of Z_0 measured on two transformers with different ratings (25 kVA and 25 MVA) are shown in Fig. 4 and compared to results of simulation in [36].

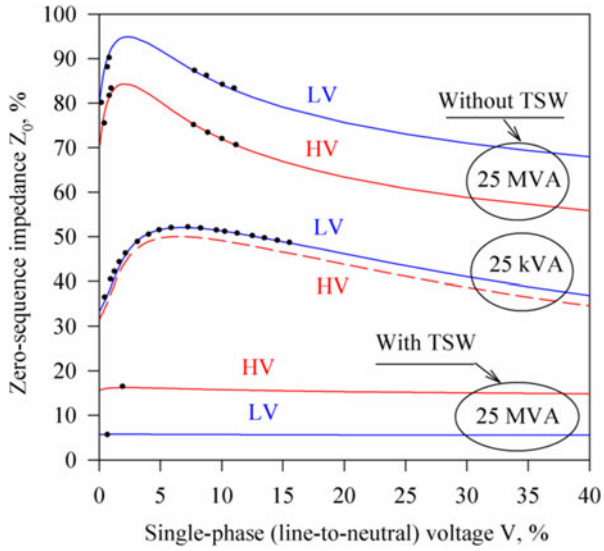

Fig. 4. Variation of the zero-sequence impedance of two core-type transformers with respect to the terminal voltage. Results derive from measurements are represented by dots and those from EMTP simulations with lines [36]. TSW = Tertiary Stabilizing Winding.

The relatively small influence of the tank in five-legged transformers and in the presence of delta winding is explained in [37]. It is important to distinguish between the *magnetizing* (open circuit) Z_0 and the *leakage* (short circuit) Z_0. The open circuit zero sequence impedance is measured with all other windings open-circuited. However, the short circuit zero sequence impedance is determined when one of the other windings is short-circuited [37]. The latter impedance is significantly smaller (see lower curves in Fig. 4) and can be estimated with sufficient accuracy using the analytical formulae employed for the calculation of short-circuit positive-sequence impedance. The behavior of a three-phase transformer supplied by unbalanced terminal voltages, in particular when a single-phase fault occurs nearby is largely determined by the transformer zero-sequence impedance Z_0.

A delta winding behaves as a short circuit path for zero sequence ac currents. This means that the zero sequence ac flux does not escape the area in-between the windings. The ac zero sequence currents circulate in the delta, thus the core will not become saturated (all zero sequence flux becomes leakage flux). As a result, the effect of the tank is insignificant in the presence of a delta connected winding with only ac excitation. However, in cases with dc bias such as GIC, dc flux may penetrate the tank even when a delta winding is present. Therefore, the tank, the shunts, and the structural parts made of steel can saturate under certain conditions and need to be modeled [16]. The transformer tank significantly impacts the zero-sequence characteristics due to its nonlinear hysteretic behavior confirmed by measurements in [32]. The dc (stray) flux may saturate different parts of the tank, shunts, and other structural components, which would affect the excitation current and reactive power. However, modeling this nonlinear return path is not trivial, since stray flux is not confined to predefined flux tubes (or paths) [29].

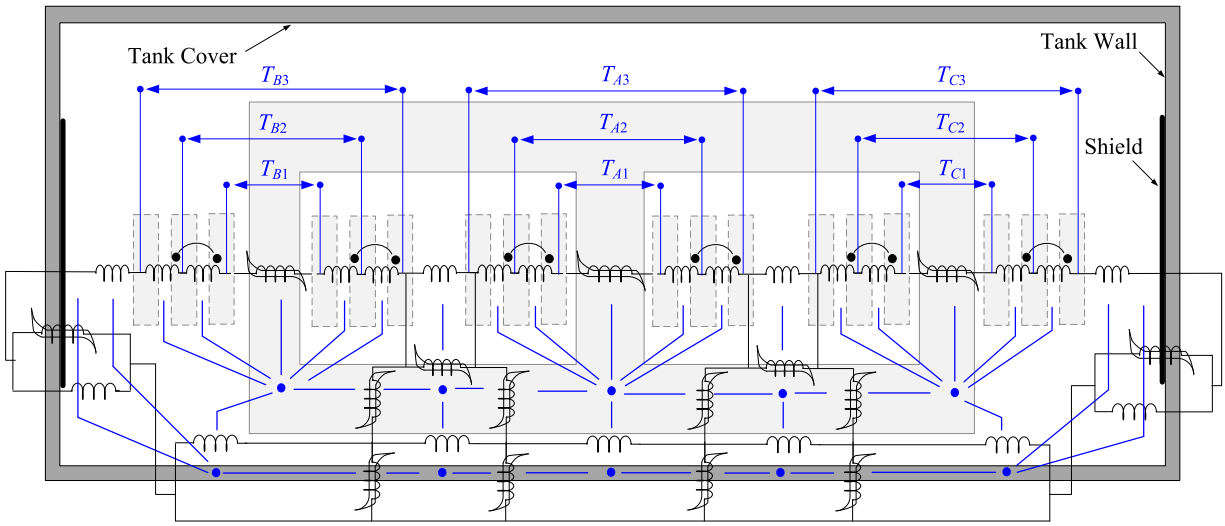

Fig. 5. Core and winding arrangement and corresponding dual electric circuit for a three-winding three-limb transformer with mutual couplings for the leakage.

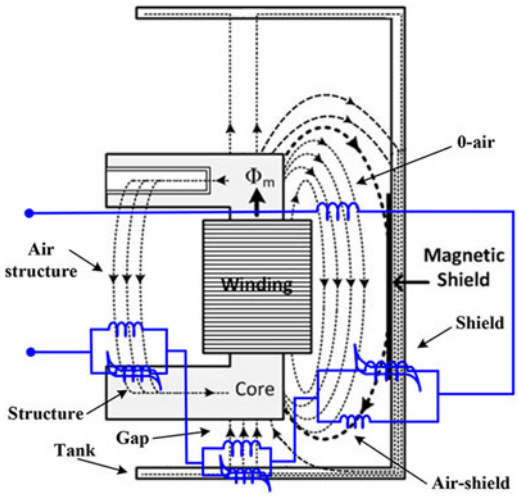

Fig. 6. Stray flux paths and dual model.

In five-legged or shell-type geometries, the zero sequence flux closes over the side legs. Therefore, under normal and unbalanced conditions the flux hardly penetrates the tank.

The dual transformer model in the presence of the tank is a 3D reluctance (dual inductance) network, because of the various possible paths of flux during the saturation of the transformer core. The behavior of the tank complicates the creation of a general topological model for three-leg transformers, since the return path will be also affected by the location of shunts and materials used. There exists some very complex models, such as the one presented in [38], with a number of inaccuracies and limitations. Alternatively, [34], [39], [40] have used simple 3D reluctance models that also take into account the flux path through air and transformer tank, which can reasonably account for the tank impact using simple electric-magnetic model, specifically for three legged cores.

In the technical literature, there are very few transformer models for electromagnetic transients which explicitly represent the tank in the transformer model, [16], [32], [41]–[43]. However, some of these models have limitations, which are mainly due to the traditional representation of the transformer zero-sequence impedance as either a linear or a nonlinear inductance in parallel with a power loss resistance.

The non-laminated tank is the main origin of the power loss in the case of unbalanced operating conditions. This is due to the induced eddy currents in the tank which are a frequency-dependent phenomenon. Therefore, the determination of the transformer tank effects at one frequency (e.g., power frequency [43]) is not valid for transient studies. A more accurate transformer model is needed to properly account for the frequency-dependent behavior of the tank.

Recent transformer models taking into account the tank are given in [36] and [16], [41]. These two tank models are introduced below, and their scopes and limitations are discussed.

1) Tank Model From [16], [41]: Fig. 5 shows the core and winding arrangement of a three-winding three-leg transformer. The electrical equivalent circuit is derived from the direct application of the principle of duality superimposed on the transformer frame. The iron properties of core and tank are modeled by means of hysteretic characteristics. The air-path fluxes are represented by linear inductances. Double-sided mutual couplings are used to model the leakage flux paths, but the negative inductance model can be also applied (as shown in Part I, these models are mathematically equivalent, for three-winding transformers).

The parameters of the equivalent circuit of Fig. 5 can be obtained from the test data. However, the determination of all parameters based on the measurements is not trivial. Therefore, an average model is presented in [16] which facilitates the parameter determination based on the test data.

The zero-sequence equivalent of this model is obtained from the application of the principle of duality on the stray fluxes as shown in Fig. 6. A part of the air flux crosses the upper and lower air gaps with the equivalent inductance L_{gap} and closes its path through the tank represented by L_{tank}. A portion of the

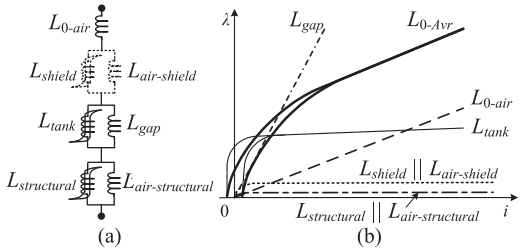

Fig. 7. Derivation of the equivalent magnetization characteristic (a) electric equivalent circuit derived from Fig. 6, (b) DC magnetization characteristic of the equivalent circuit of Fig. 5.

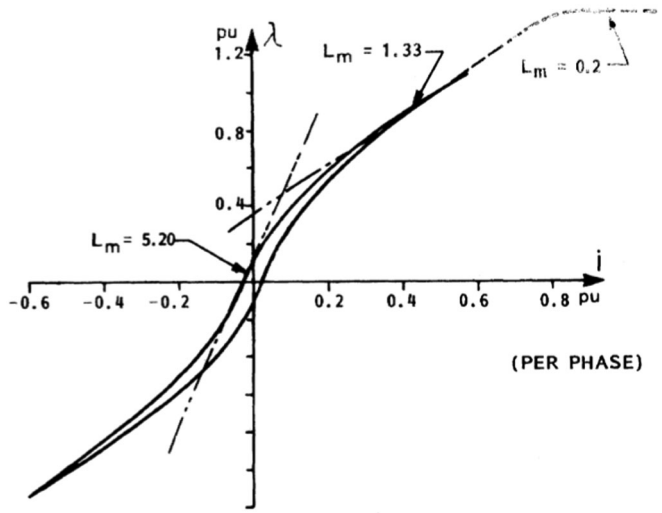

Fig. 8. Measured zero-sequence magnetization characteristic of a 25 MVA 110/44/4 kV three-limb core type transformer [32].

flux links with the tank magnetic shield if such a shield exists in the construction of the transformer. The shield and the air path of the corresponding linking flux are represented by $L_{\rm shield}$ and $L_{\rm air\text{-}shield}$, respectively. Similarly, the clamping structural components and the associated air path fluxes are denoted by $L_{\rm structural}$ and $L_{\rm air\text{-}structural}$, respectively. The other part of the flux is entirely in air and thus can be modeled by $L_{0\text{-}\rm air}$.

Fig. 7(a) shows the equivalent circuit associated with the flux paths of Fig. 6. The nonlinear tank iron, the magnetic shield and the magnetic structural part should be represented by means of dynamic hysteretic models. Depending on the operating conditions, for example at power frequency, using the single-valued characteristics of the tank iron rather than the hysteretic ones provides sufficiently accurate results [41].

The parameters of the equivalent circuit of Fig. 7(a) can be obtained from the characteristics of the curves of Fig. 7(b) and a zero-sequence dc test. The dc test on a 25 MVA 110/44/4 kV three-leg core-type transformer is illustrated in Fig. 8 [32]. The characteristic of Fig. 7(b) can be simplified to Fig. 8 when the magnetic shield effects are neglected. The slopes at the higher and the lower excitation levels corresponds to $L_{0\text{-}\rm air}$ and $L_{0\text{-}\rm air} + L_{\rm gap}$, respectively. $L_{0\text{-}\rm air}$ is close to the standard zero-sequence data. However, the determination of $L_{\rm gap}$ is difficult

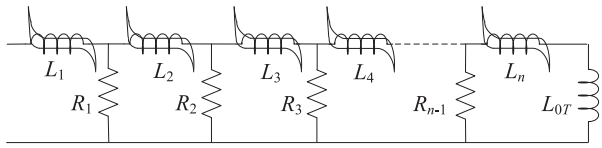

Fig. 9. Cauer circuit representing a central belt of the tank walls. Note that, all L and R parameters can be assumed to be equal. For this, $L_1 = L_{\rm n} = L/2$, $L_2 = L_3 = \ldots L_{n-1} = L$, and $R_1 = R_2 = \ldots = R_{n-1} = R$.

due to non-uniform air-gap and the fringing flux pattern of the air-gap.

2) Tank Model From [36]: Reference [36] introduces an improved model to represent zero-sequence impedance of a three-leg transformer. The transformer model is based on the fact that the zero-sequence impedance is altered by the change of voltage or current magnitude in the standard zero-sequence test [37], [44], [45]. In [44], the variation of the measured zero-sequence impedance of a 45/16.05/10 kV–25 MVA transformer with the applied voltage is presented. Measurement results are compared with the results obtained from the corresponding transformer models.

To reproduce the zero-sequence impedance $\underline{Z}_0\,(V)$ of Fig. 4, the central belt of the tank walls can be represented with a Cauer circuit (Fig. 9) [36]. In this figure, R is the resistance of a wall "layer" that reproduces the losses in the corresponding layers. The saturable inductances L_n can be modeled either as hysteretic or with a single-valued nonlinear characteristic. Inductance L_{0T} represents the space beyond the tank and is an auxiliary element which plays a role only in deep saturation of the tank. Parameters of the Cauer circuit are specified in [36] where the circuit with 25 sections (layers) was employed.

The distinguishing feature of the transformer model of [36] is that the eddy currents of the tank walls enclose all three wound legs of the core making the walls an equivalent delta winding [37].

The three-legged 25 MVA unit studied in [36] has no magnetic shunts. Therefore, its tertiary stabilizing winding (TSW) can be open or closed. In the case of the closed delta winding, the model reproduces correctly the decrease of Z_0 observed in the experiment. The simulation results are shown by solid lines in Fig. 4.

The capabilities of the transformer model of [36] in studying GIC events are illustrated in Figs. 10 and 11. To reproduce GIC, a dc step voltage ($V = -22.8$ V) is applied at $t = 0.1$ s on the HV neutral point. At this instant, the currents in the windings start to increase reaching 100 A/phase GIC in steady-state. Fig. 10 shows transient and steady-state currents calculated in the absence of the TSW. The influence of the TSW on the magnetic fields at the inner and outer surfaces of the tank wall is shown in Fig. 11. The effect can be seen when comparing Figs. 10 and 11.

3) Discussion: Some of the special characteristics of the tank structure when facing transients still need research, since there is no consensus among the researchers. For example, [36] introduces the saturation of the tank layers as the cause of the zero-sequence impedance variation. However, the model of [16]

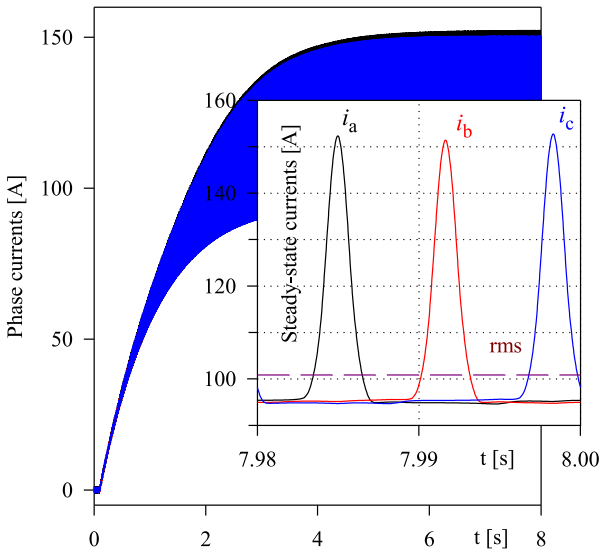

Fig. 10. Phase GICs of a three-legged transformer calculated in the absence of the TSW.

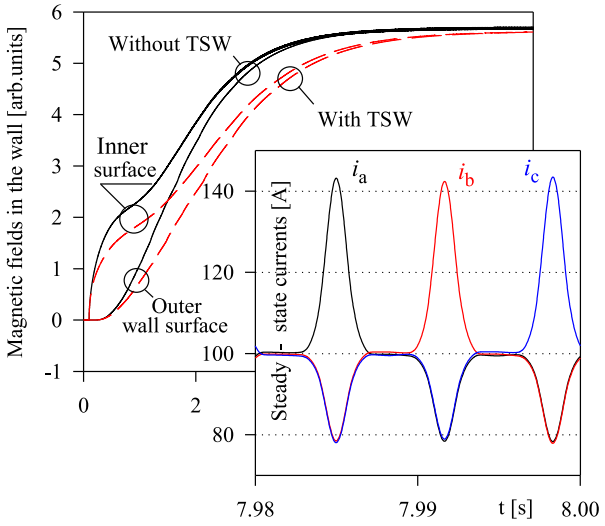

Fig. 11. The influence of the TSW on the magnetic fields in the tank walls and GICs of a three-legged transformer.

reports that the variation is due to the magnetic structural parts (e.g., core tie-plate) and exhibits a noticeably lower saturation level at power frequency, i.e., about 0.02 pu, as compared with the tank saturation level. The actual saturation level of the structural parts obtained from a dc excitation can be higher. However, lower saturation levels at power frequency have been observed which is due to the establishment of eddy currents in these parts. The phenomenon prevents further penetration of flux which results in a characteristic similar to saturation [41], [46]. Note that, these conclusions may change for transformers with different structures. It may be the tank, the core frame, the frame tie rods, or the shunts, that saturate first depending on the construction details of the transformer.

Other important issue is the modeling of the zero sequence impedance and losses because of the impacts of the tank and magnetic structural parts at different frequencies. Reference [16] reports that based on the topological equivalent of the air-gap, tank, and the core structural part, replication of such impedance variations can be achieved. This is why the results in [36] show that a ladder-type Cauer circuit is needed to model the layer-by-layer saturation of the tank that represents this behavior.

As discussed before, the effect of the transformer tank is significant in over-excitation and zero-sequence conditions. Some of the models are specialized to represent a particular regime. For example, the model presented in [36] performs satisfactorily for zero-sequence conditions; however, it needs to be tested for zero-sequence power loss, global saturation of the tank under balanced over-excitation, or local saturation of the transformer tank for unbalanced over-excitations.

Other alternatives are the models presented in [11] and [29]. The determination of parameters is still a challenge, but efforts are under way to obtain all model parameters from terminal measurements.

VI. Modeling Guidelines

It is not always necessary to consider all parameters in a transformer model for a specific study. For example, capacitive effects may be negligible for some transient studies while they may be significant for others. The iron core may either be ignored, be represented with a constant inductor, a saturation curve, a static hysteresis model, or a dynamic hysteresis model. The windings could be modeled in great details to include the frequency dependent behavior of the resistance and leakage inductance, or as bulk elements.

There are different opinions about the importance of a dynamic hysteresis model for certain transients. Some references show that the representation of the dynamic hysteresis is important in GIC and ferroresonance studies. The frequency dependency of the core and the tank iron has impacts on the GIC as well [16], [41]. Also, the accurate estimation of power loss from a dynamic hysteresis model may be significant in the determination of the transformer thermal behavior [47]. For ferroresonance studies, hysteresis can noticeably influence the simulation results due to two main aspects: core loss and core dynamic inductance [48]. It is widely known that the core loss plays a significant role in the constitution of ferroresonance. However, the simulation results of [49], [50] reveal that the effect of hysteresis cannot be limited to its power loss aspect. Different formation of the hysteresis minor loops can significantly influence ferroresonance and the stability domains of the various ferroresonance modes, as shown in [50]. This is so because the hysteretic and even the non-hysteretic models can give a significantly different core dynamic inductance [48].

Fig. 12 shows ferroresonance simulation results for the 3-legged transformer of [44] based on the transformer model of [16] and [41] with static and dynamic hysteresis models. It is assumed that the no-load transformer is supplied through a series 0.35 μF capacitance and the voltage source of 45 kV (1 pu), 60 Hz. Due to higher losses resulting from the dynamic hysteresis, the ferroresonance oscillation is a sustained fundamental mode with the magnitude of about 1.75 pu, whereas due to lower

TABLE II
GUIDELINES FOR THE REPRESENTATION OF THE MODEL COMPONENTS FOR DIFFERENT LOW-FREQUENCY STUDIES

Study type	Core	Windings	Capacitive effects	Tank
Inrush currents	Piecewise linear with two slopes[1]	Bulk leakage Bulk resistance	Negligible	Important
Ferroresonance	Dynamic hysteresis	Bulk leakage Bulk resistance	Important	Important
GIC	Piecewise linear with two slopes	Bulk leakage Bulk resistance	Negligible	Important
Harmonic penetration	Dynamic hysteresis	Eddy effects with Physical Cauer	Negligible	Negligible
Calculation of losses and reactive power	Bulk losses	Eddy effects with Physical Cauer	Negligible	Important
De-energization	Dynamic hysteresis	Bulk leakage Bulk resistance	Important	Negligible

[1]Piecewise linear is adequate for energization, but dynamic hysteresis is recommended to compute the residual flux from the previous de-energization.

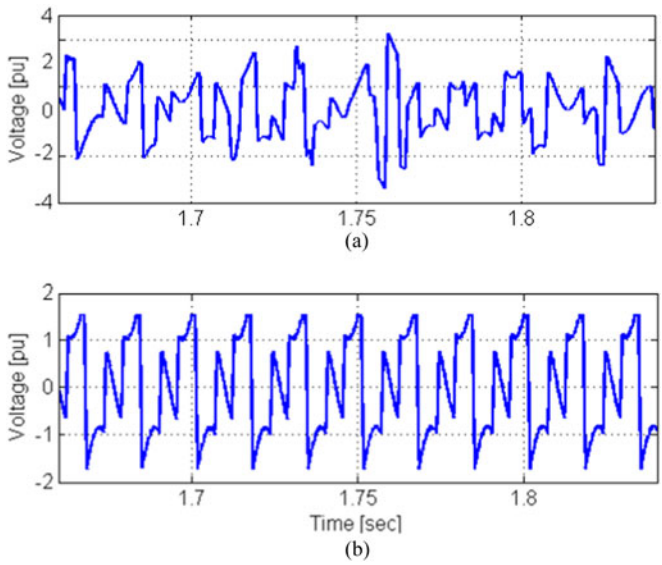

Fig. 12. Terminal voltage of a three-leg transformer with: (a) static hysteresis model; (b) dynamic hysteresis model.

damping of the static hysteresis model, the associated simulation results shows a chaotic ferroresonance with the magnitude exceeding 3.0 pu.

In contrast, some experts believe that the dynamic hysteresis is not of practical importance in the GIC performance. Hysteresis may have some noticeable influence at very low levels of GIC, but these effects are benign and are not of much interest. At higher current levels there is the concern of transformer heating. Under these conditions hysteresis has a negligible impact and can be ignored with no practical detriment to the results. Under GIC and inrush conditions the most effective parameters are the saturation inductance and the saturation level of the transformer iron-core [51].

For inrush current transients, modeling the residual flux of the hysteretic core is a fundamental requirement, especially when multi energizations of transformer need to be investigated. Also, hysteresis minor loops are significant for the calculation of inrush or ferroresonance when the residual flux needs to be considered properly. However, simulation results show that if the residual flux is known, hysteresis models are not needed and a piecewise linear inductance is adequate. This nonlinear inductance can be constructed of several pieces (practically 2 to 10), where the final slope shall be the "saturation inductance." Experience shows that a two slope model and the availability of the residual flux as the initial condition, suffices to predict inrush currents [52]. This is so because for inrush currents, the transformer is driven to deep saturation (higher than 2.0–2.2 Tesla). In moderate saturation levels, when the flux density does not exceed 1.9–2.0 Tesla, a nonlinear inductor with more accuracy (multi-section) is desirable. Note that, it is critical to identify the proper saturation level (bending point), when approximating the magnetizing characteristic with two slopes [53].

Capacitive effects are not negligible for ferroresonance studies especially for large power transformers. Field experience has shown that ferroresonance may happen solely because of the resonance between the transformer winding capacitance and the transformer magnetizing characteristic. Capacitive effects can also be very important to model the demagnetization process and to determine the residual flux in the core after disconnection.

There is no transformer model yet capable of predicting accurately and consistently the residual flux following transformer de-energization. In addition to the modelling complexities of the magnetic material, other parameters such as air-gaps in the T-joints need to be accurately measured and modeled. Interesting attempts to estimate the residual flux following a transformer disconnection are presented in [27] and [54].

Table II provides a guideline to select necessary elements to be modeled for various low-frequency transient studies. To model the windings, the Mutual Coupling (MC), the Negative Inductance, or the BCTRAN models described in Part I can be used as a bulk leakage representation of transformers up to three-windings. For transformers with more than three windings, the MC and the BCTRAN models are more accurate (see Part I). To consider eddy current effects in the windings (frequency dependent resistance and inductance), the model presented in [11] is recommended. One of the models presented in [16] and [36] may be utilized for the tank. Capacitive effects between the windings and winding layers can be considered according to [11].

VII. CONCLUSION

Transformer models have been reviewed and classified into three categories based on the required information and the applicable identification methods. Gray-box models seem to be more practical with sufficient engineering accuracy when compared with black- and white-box models. The determination of model parameters remains a major issue that requires improvements in the standard tests.

Static and dynamic hysteresis models have been critically reviewed. The importance of the proper inclusion of iron core losses, especially excess losses, to model the magnetic material has been discussed.

The significance of an accurate tank model to simulate transformers under unbalanced and over-excitation conditions has been highlighted. Currently available tank models as well as their scope and limitations have been reviewed. It is evident that there are still unresolved issues in the area of the tank modeling, and this can be a challenging subject for future research.

The important parameters for different operating regimes and electromagnetic transient events have been identified. Accordingly, guidelines have been presented for power system modelers for the efficient and accurate modeling of the transformers for low-frequency transients. These guidelines should help the transformer modeler to simulate the transformer behavior sufficiently close to reality with the minimum computational effort.

Model examples for a single-phase shell-type transformer with two and three-windings have been offered in Part I. In Part II, a three-phase general model has been produced for a core-type transformer. Note that, the models presented are "unified models" which are accurate for all low frequency transients for the given transformer topology.

REFERENCES

[1] J. A. Martinez and B. A. Mork, "Transformer modeling for low- and mid-frequency transients—A review," *IEEE Trans. Power Del.*, vol. 20, no. 22, pp. 1625–1632, Apr. 2005.

[2] S. D. Mitchell and J. S. Welsh, "Initial parameter estimates and constraints to support gray box modeling of power transformers," *IEEE Trans. Power Del.*, vol. 28, no. 4, pp. 2411–2418, Oct. 2013.

[3] B. Gustavsen, "Wide band modeling of power transformers," *IEEE Trans. Power Del.*, vol. 19, no. 1, pp. 414–422, Jan. 2004.

[4] B. Gustavsen, "Wide-band transformer modeling including core nonlinear effects," *IEEE Trans. Power Del.*, vol. 31, no. 1, pp. 219–227, Feb. 2016.

[5] X. Lopez-Fernandez and C. Alvarez-Mariño, "Computation method for transients in power transformers with lossy windings," *IEEE Trans. Magn.*, vol. 45, no. 3, pp. 1863–1866, Mar. 2009.

[6] S. Jazebi, F. de León, and B. Vahidi, "Duality-synthesized circuit for eddy current effects in transformer windings," *IEEE Trans. Power Del.*, vol. 28, no. 2, pp. 1063–1072, Apr. 2013.

[7] E. J. Tarasiewicz, A. S. Morched, A. Narang, and E. P. Dick, "Frequency dependent eddy current models for nonlinear iron cores," *IEEE Trans. Power Syst.*, vol. 8, no. 2, pp. 588–597, May 1993.

[8] F. de León and A. Semlyen, "Complete transformer model for electromagnetic transients," *IEEE Trans. Power Del.*, vol. 9, no. 1, pp. 231–239, Jan. 1994.

[9] P. G. Blanken, "A lumped winding model for use in transformer models for circuit simulation," *IEEE Trans. Power Electron.*, vol. 16, no. 3, pp. 445–460, May 2001.

[10] T. Prevost and D. Woodcock, "Transformer fleet health and risk assessment," presented at the *IEEE Power Eng. Soc. Transformers Committee Tutorial*, Dallas, TX, USA, 2007.

[11] S. Jazebi and F. de León, "Duality-based transformer model including eddy current effects in the windings," *IEEE Trans. Power Del.*, vol. 30, no. 5, pp. 2312–2320, Oct. 2015.

[12] S. Jazebi, F. de León, A. Farazamand, and D. Deswal, "Dual reversible transformer model for the calculation of low-frequency transients," *IEEE Trans. Power Del.*, vol. 28, no. 4, pp. 2509–2517, Oct. 2013.

[13] S. Jazebi and F. de León, "Experimentally validated reversible single-phase multi-winding transformer model for the accurate calculation of low-frequency transients," *IEEE Trans. Power Del.*, vol. 30, no. 1, pp. 193–201, Feb. 2015.

[14] B. A. Mork, F. Gonzalez, D. Ishchenko, D. L. Stuehm, and J. Mitra, "Hybrid transformer model for transient simulation—Part I: Development and parameters," *IEEE Trans. Power Del.*, vol. 22, no. 1, pp. 248–255, Jan. 2007.

[15] S. Mitchell and J. Welsh, "Modeling power transformers to support the interpretation of frequency-response analysis," *IEEE Trans. Power Del.*, vol. 26, no. 4, pp. 2705–2717, Oct. 2011.

[16] A. Rezaei-Zare, "Enhanced transformer model for low-and mid-frequency transients—Part I: Model development," *IEEE Trans. Power Del.*, vol. 30, no. 1, pp. 307–315, Feb. 2015.

[17] K. Foster, F. E. Werner, and R. M. Del Vecchio, "Loss separation measurements for several electrical steels," *J. Appl. Phys.*, vol. 53, pp. 8308–8310, Nov. 1982.

[18] G. Bertotti, *Hysteresis in Magnetism: For Physicists, Materials Scientists, and Engineers*, San Diego, CA, USA : Academic Press, 1998.

[19] S. E. Zirka, Y. I. Moroz, A. J. Moses, and C. M. Arturi, "Static and dynamic hysteresis models for studying transformer transients," *IEEE Trans. Power Del.*, vol. 26, no. 4, pp. 2352–2362, Oct. 2011.

[20] J. Avila-Rosales and F. L. Alvarado, "Nonlinear frequency dependent transformer model for electromagnetic transient studies in power systems," *IEEE Trans. Power App. Syst.*, vol. PAS-101, no. 11, pp. 4281–4288, Nov. 1982.

[21] S. E. Zirka, Y. I. Moroz, N. Chiesa, R. G. Harrison, and H. Kr. Hoidalen, "Implementation of inverse hysteresis model into EMTP—Part I: Static model," *IEEE Trans. Power Del.*, vol. 30, no. 5, pp. 2224–2232, Oct. 2015.

[22] D. C. Jiles and D. L. Atherton, "Theory of ferromagnetic hysteresis," *J. Appl. Phys.*, vol. 55, pp. 2115–2120, Mar. 1984.

[23] F. Preisach, "Uber die magnetische nachwerikung," *Zeitschrift Phys.*, vol. B 94, pp. 227–302, 1935.

[24] F. de Leon, and A. Semlyen, "A simple representation of dynamic hysteresis losses in power transformer," *IEEE Trans. Power Del.*, vol. 10, no. 1, pp. 315–321, Jan. 1995.

[25] S. E. Zirka, Y. I. Moroz, P. Marketos, A. J. Moses, D. C. Jiles, and T. Matsuo, "Generalization of the classical method for calculating dynamic hysteresis loops in grain-oriented electrical steels," *IEEE Trans. Magn.*, vol. 44, no. 9, pp. 2113–2126, Sep. 2008.

[26] S. E. Zirka, Y. I. Moroz, N. Chiesa, R. G. Harrison, and H. Kr. Hoidalen, "Implementation of inverse hysteresis model into EMTP—Part II: Dynamic model," *IEEE Trans. Power Del.*, vol. 30, no. 5, pp. 2233–3241, Oct. 2015.

[27] H. Kr. Høidalen, A. Lotfi, S. E. Zirka, Y. I. Moroz, N. Chiesa, and B. A. Mork, "Benchmarking of hysteretic elements in topologically correct transformer model," in *Proc. Int. Conf. Power Syst. Transients*, 2015, pp. 15–18.

[28] X. Chen and P. Neudorfer, "Digital modeling of modern single-phase distribution transformers," in *Proc. Inst. Elect. Eng., Int. Conf. Power Syst. Control, Oper., Manage.*, 1991, pp. 914–920.

[29] M. Lambert and J. Mahseredjian, *Electromagnetic Transient-Type Transformer Models for Geomagnetically-Induced Current (GIC) Studies* EPRI, Palo Alto, CA, Pub. ID: 3002000832, 20 Nov. 2013.

[30] C. M. Arturi, "Model of a highly saturated three-phase autotransformer with tertiary winding and five-limb core and analysis of a time-varying short-circuit transient," *Eur. Trans. Elect. Power*, vol. 4, no. 6, pp. 513–524, Nov./Dec. 1994.

[31] F. de León, S. Jazebi, and A. Farazmand, "Accurate measurement of the air-core inductance of iron-core transformers with a non-ideal low-power rectifier," *IEEE Trans. Power Del.*, vol. 29, no. 1, pp. 294–296, Feb. 2014.

[32] E. P. Dick and W. Watson, "Transformer models for transient studies based on field measurements," *IEEE Trans. Power App. Syst.*, vol. PAS-100, no. 1, pp. 409–419, Jan. 1981.

[33] C. G. A. Koreman, "Determination of the magnetizing characteristic of three-phase transformers in field tests," *IEEE Trans. Power Del.*, vol. 4, no. 3, pp. 1779–1785, Jul. 1989.

[34] S. Abdulsalam, W. Xu, W. L. A. Neves, and X. Liu, "Estimation of transformer saturation characteristics from inrush current waveforms," *IEEE Trans. Power Del.*, vol. 21, no. 1, pp. 170–177, Jan. 2006.

[35] S. Calabro, F. Coppadoro, and S. Crepaz, "The measurement of the magnetizing characteristics of large power transformers and reactors through d.c. excitation," *IEEE Trans. Power Del.*, vol. PWRD-1, no. 4, pp. 224–234, Oct. 1986.

[36] S. E. Zirka, Y. I. Moroz, and C. M. Arturi, "Accounting for the influence of the tank walls in the zero-sequence topological model of a three-phase, three-limb transformer," *IEEE Trans. Power Del.*, vol. 29, no. 5, pp. 2172–2179, Oct. 2014.

[37] S. V. Kulkarni and S. A. Khaparde, *Transformer Engineering: Design and Practice*, New York, USA: Marcel Dekker, 2004.
[38] J. Turowski, M. Turowski, and M. Kopec, "Method of three-dimensional network solution of leakage field of three-phase transformers," *IEEE Trans. Magn.*, vol. 26, no. 5, pp. 2911–2919, Sep. 1990.
[39] M. Elleuch and M. Poloujadoff, "A contribution to the modeling of three phase transformers using reluctances," *IEEE Trans. Magn.*, vol. 32, no. 2, pp. 335–343, Mar. 1996.
[40] M. Elleuch and M. Poloujadoff, "Anisotropy in three-phase transformer circuit model," *IEEE Trans. Magn.*, vol. 33, no. 5, pp. 4319–4326, Sep. 1997.
[41] A. Rezaei-Zare, "Enhanced transformer model for low and mid-frequency transients—Part II: Validation and simulation results," *IEEE Trans. Power Del.*, vol. 30, no. 1, pp. 316–325, Feb. 2015.
[42] A. Narang and R. H. Brierley, "Topology based magnetic model for steady-state and transient studies for three phase core type transformers," *IEEE Trans. Power Syst.*, vol. 9, no. 3, pp. 1337–1349, Aug. 1994.
[43] E. F. Fuchs and Y. You, "Measurement of $\lambda - i$ characteristics of asymmetric three-phase transformers and their applications," *IEEE Trans. Power Del.*, vol. 17, no. 4, pp. 983–990, Oct. 2002.
[44] A. Ramos, J. C. Burgos, A. Moreno, and E. Sorrentino, "Determination of parameters of zero-sequence equivalent circuits for three-phase three-legged YNynd transformers based on onsite low-voltage tests," *IEEE Trans. Power Del.*, vol. 28, no. 3, pp. 1618–1625, Jul. 2013.
[45] *Power transformers—Application guide, First edition, 1997-10*, IEC Int. Standard 60076-8.
[46] P. Gómez and F. de León, "Accurate and efficient computation of the inductance matrix of transformer windings for the simulation of very fast transients," *IEEE Trans. Power Del.*, vol. 26, no. 3, pp. 1423–1431, Jul. 2011.
[47] L. Marti, A. Rezaei-Zare, and A. Narang, "Simulation of transformer hotspot heating due to geomagnetically induced currents," *IEEE Trans. Power Del.*, vol. 28, no. 1, pp. 320–327, Jan. 2013.
[48] A. Rezaei-Zare and R. Iravani, "On the transformer core dynamic behavior during electromagnetic transients," *IEEE Trans. Power Del.*, vol. 25, no. 3, pp. 1606–1619, Jul. 2010.
[49] A. Rezaei-Zare, R. Iravani, M. Sanaye-Pasand, H. Mohseni, and Sh. Farhangi, "An accurate hysteresis model for ferroresonance analysis of a transformer," *IEEE Trans. Power Del.*, vol. 23, no. 3, pp. 1448–1456, Jul. 2008.
[50] A. Rezaei-Zare, R. Iravani, and M. Sanaye-Pasand, "Impacts of hysteresis loop formation on stability domain of ferroresonance modes," *IEEE Trans. Power Del.*, vol. 24, no. 1, pp. 177–186, Jan. 2009.
[51] R. A. Walling and A. H. Khan, "Characteristics of transformer exciting current during geomagnetic disturbances," *IEEE Trans. Power Del.*, vol. 6, no. 4, pp. 1707–1714, Oct. 1991.
[52] N. Chiesa, H. K. Høidalen, M. Lambert, and M. M. Duró, "Calculation of inrush currents—Benchmarking of transformer models," presented at the *Int. Conf. Power Syst. Transients*, Delft, the Netherlands, Jun. 14–17 2011.
[53] S. Jazebi, F. de León, and N. Wu, "Enhanced analytical method for the calculation of the maximum inrush currents of single-phase power transformers," *IEEE Trans. Power Del.*, vol. 30, no. 6, pp. 2590–2599, Dec. 2015.
[54] N. Chiesa, B. A. Mork, and H. K. Høidalen, "Transformer model for inrush current calculations: Simulations, measurements and sensitivity analysis," *IEEE Trans. Power Del.*, vol. 25, no. 4, pp. 2599–2608, Oct. 2010.